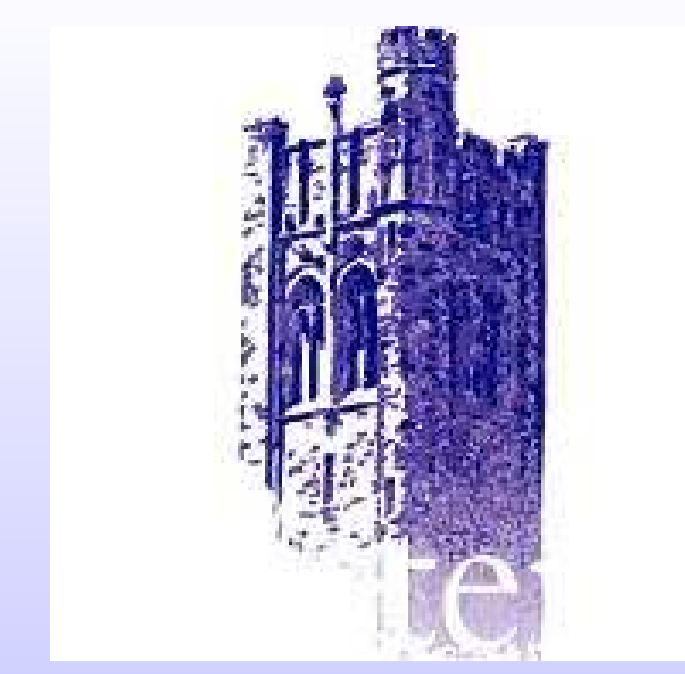


Fragmentation Mechanism of Charged Nanodroplets – A Molecular Dynamics Study

Kengo Ichiki and Styliani Consta
Department of Chemistry, University of Western Ontario



Introduction

Fragmentation of charged nanodroplets has been studied for one and a half century since Lord Rayleigh gave a stability condition[1]. In the last decades the fragmentation process has obtained practical significance because it is basic in electrospray mass spectrometry (ESMS)[2, 3, 4, 5]. About the mechanism, there are long standing arguments [6, 7, 8]. There are mainly two suggested fragmentation mechanisms, the charged residue mechanism (CRM)[9] and ion evaporation mechanism (IEM)[10]. In the former, ions are generated by successive instabilities as described by the Rayleigh theory, while in the latter, by ion evaporation treated as a first-order reaction process. Numerical study is quite important because we can observe the fragmentation event directly while in experiments the nanometer dimensions of the clusters combined with the nanosecond time scale prevent the clear observation of the fragmentation mechanism.

Molecular Dynamics Simulations

To model charged droplets in ESMS systems, constant-temperature MD by GRO-MACS version 3.2.1 [11, 12] is employed. Droplets are modeled by SPC/E model[13] for water and the force field by Chandrasekhar *et al.*[14] for Cl^- .

Solvent Evaporation: A molecule whose distance from the center of mass becomes larger than **10 nm** is excluded from the simulation.

Ion Fragmentation: We define an atom to belong to a fragment by the criterion that the atom-atom distance in that fragment is less than **1 nm**. The largest fragment is called the **main** droplet and the smaller droplets containing ions are called the **daughter** droplets.

N and z are the numbers of water molecules and ions (in the main droplet). N^* is the critical size at the fragmentation event. Radius of the main droplet is estimated by $R = (3V/4\pi)^{1/3} - R_p$, where V is the solvent accessible volume[15] with the probe of radius $R_p = 0.14$ nm calculated by the program called “spacefill” in TINKER[16].

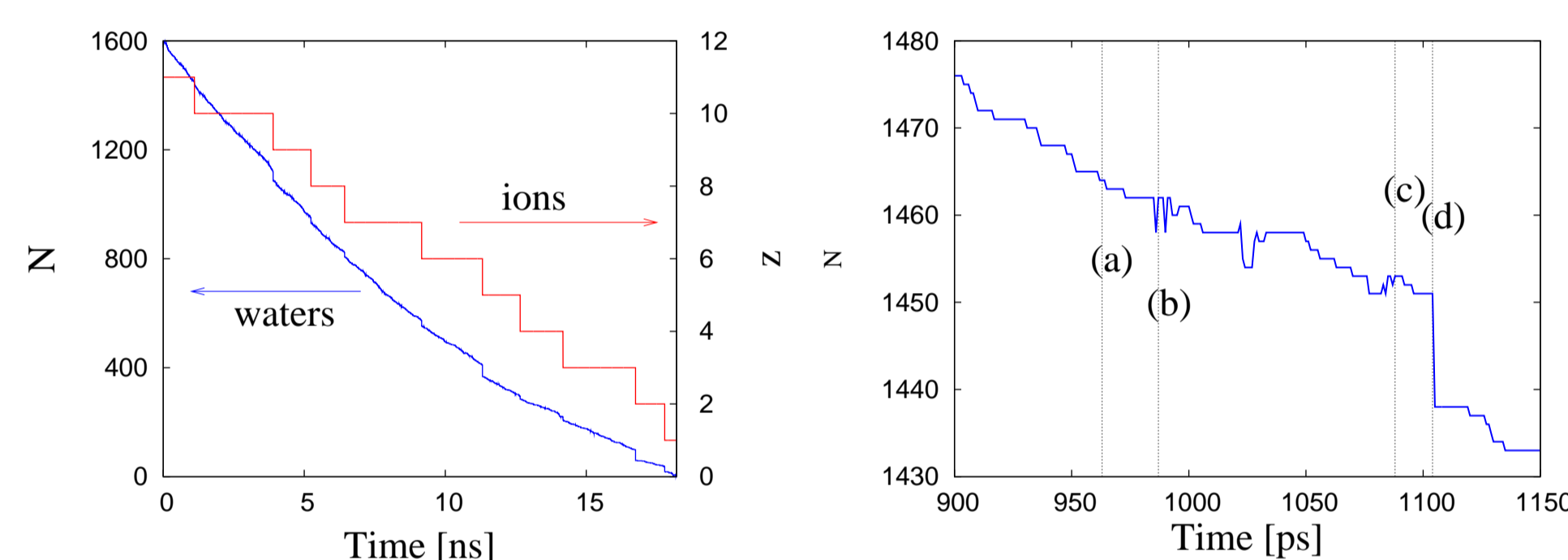


FIGURE 1: A sequence of fragmentation events in a simulation at $T = 350$ K. The blue line represents the variation of N in the main droplet and the red line the variation of z also in the main droplet. The marked configurations (a)-(d) correspond to the snapshots given in Fig. 2.

Single-ion fragmentation is dominant. We find only 6 events of two-ion fragmentation out of 133 total fragmentation events. The critical sizes N^* are hardly affected by the history of solvent evaporation when the evaporation and fragmentation rate are slow, but are well determined by z and T .

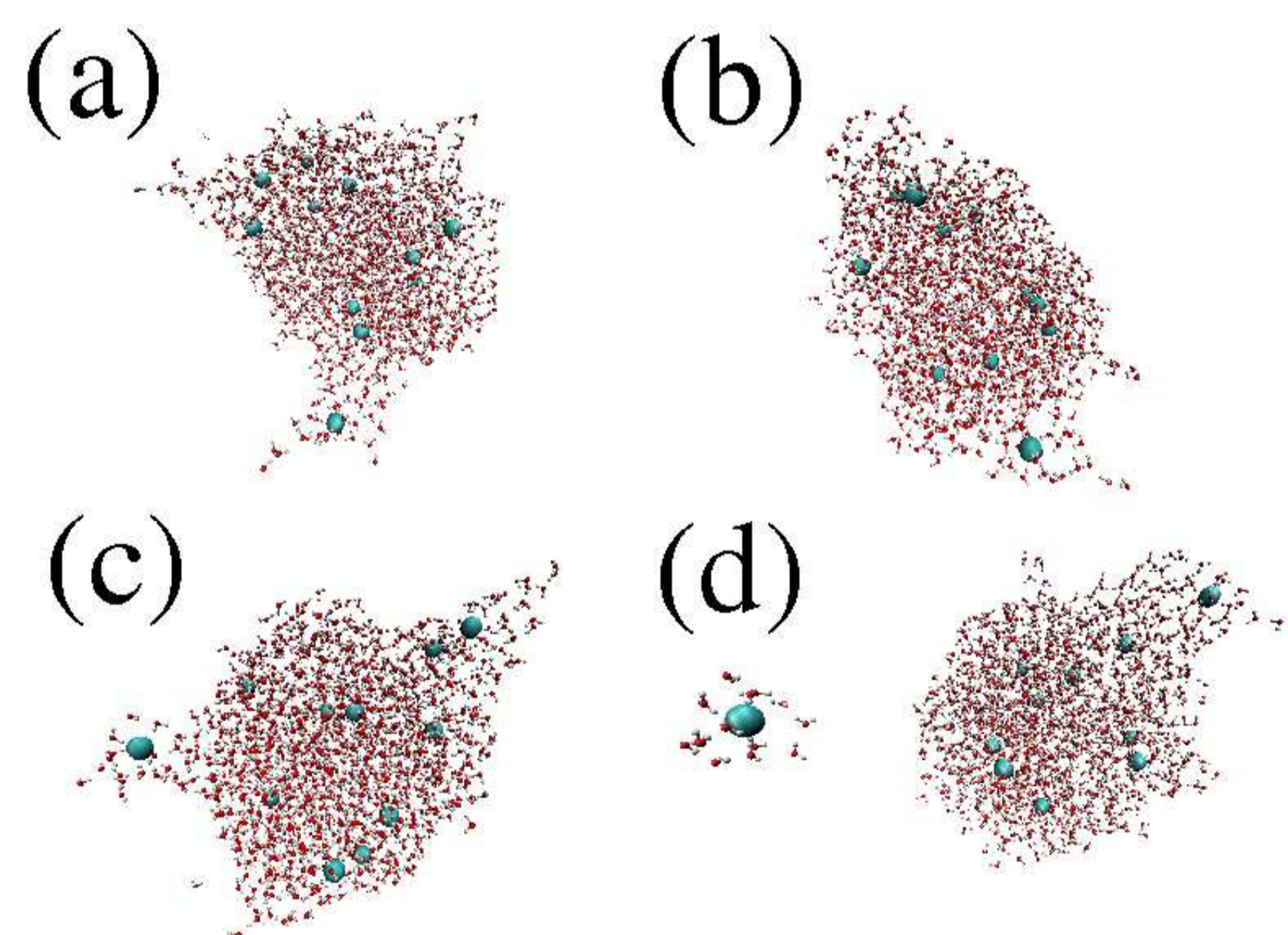


FIGURE 2: Snapshots from simulation in Fig. 1. The blue spheres represent the Cl^- and water molecules are drawn by red and white spheres. (a), (b), (c) and (d) are shown in Fig. 1. In (d) the daughter droplet contains an ion and 13 water molecules.

- (a) The left- and right-top regions of the droplet are the thorns without ion, while the bottom region is that with an ion.
- (b) The thorn with an ion does not disintegrate on this occasion and the ion returns to the main droplet.
- (c) There is the thorn with an ion again.
- (d) It eventually departs from the main droplet.

We define the *critical* radius $R^*(z)$ as the minimum radius of the droplet holding z ions.

Rayleigh Theory

Lord Rayleigh[1] argued the shape instability of a charged droplet and gave the famous relation for the critical radius as

$$R_R(z) = \left(\frac{e^2 z^2}{64\pi^2 \epsilon_0 \gamma} \right)^{1/3}, \quad (1)$$

where e is the elementary charge, ϵ_0 is the permittivity of vacuum, γ is the surface tension of the solvent. We use $\gamma(T)$ for bulk water given by the International Association for the Properties of Water and Steam[17].

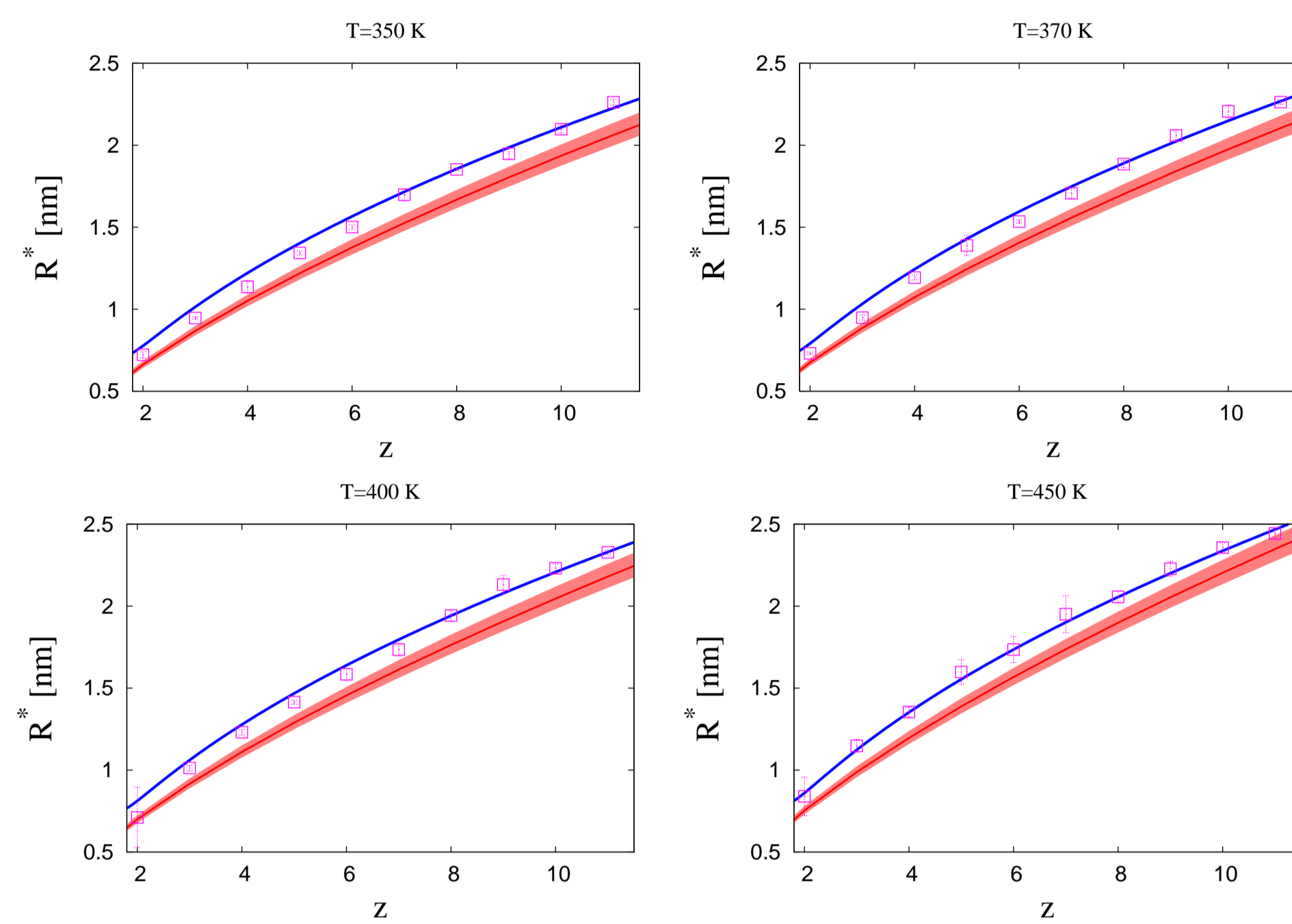


FIGURE 3: The critical radius $R^*(z)$ at $T = 350, 370, 400,$ and 450 K is shown by pink marks. Red and blue lines correspond to Rayleigh theory (1) and the simplified IEM (6), respectively. The red region around the Rayleigh theory denotes uncertainty due to γ .

The agreement of Rayleigh’s theory on R^* is relatively good. However, we do not support Rayleigh’s theory for the fragmentation mechanism, because the assumptions in the theory is not valid for the simulations:

- The shape of the droplet are far from the spherical shape,
- The uniform charge distribution on the surface is never attained.

Potential Energy

As shown in Fig. 4, the fragmentation requires the system to overcome a potential energy barrier. This suggested that the process is activated and that a mechanism more along the lines of IEM is more favorable.

Born Theory

The reversible work to move a cluster with radius R_d containing a solvation ion from the liquid to vacuum (the Gibbs free energy) is given by

$$\Delta^\circ = \frac{e^2}{8\pi\epsilon_0 R_d} + 4\pi\gamma R_d^2. \quad (2)$$

This free energy Δ° has the minimum value ΔG_S° at the Born radius

$$R_B = \left(\frac{e^2}{64\pi^2 \epsilon_0 \gamma} \right)^{1/3}. \quad (3)$$

R_d and N_d in the simulations are compared with R_B and the hydration numbers N_h . The averages of R_d and N_d are larger than R_B and N_h , respectively. But for both cases, the minimum values seem to correspond to R_B and N_h . This may be explained by the following:

- The cluster of ion with the hydration shell is the unit in the main droplet.
 - Sometimes it starts detaching from the main droplet as in Fig. 2 (a) and (c) making a bridge of water molecules.
 - The cluster may leave the main droplet pinching at certain point in the bridge as in (d).
- Therefore, the daughter droplet consists of the ion with the hydration shell and some portion of the water molecules in the bridge structure.

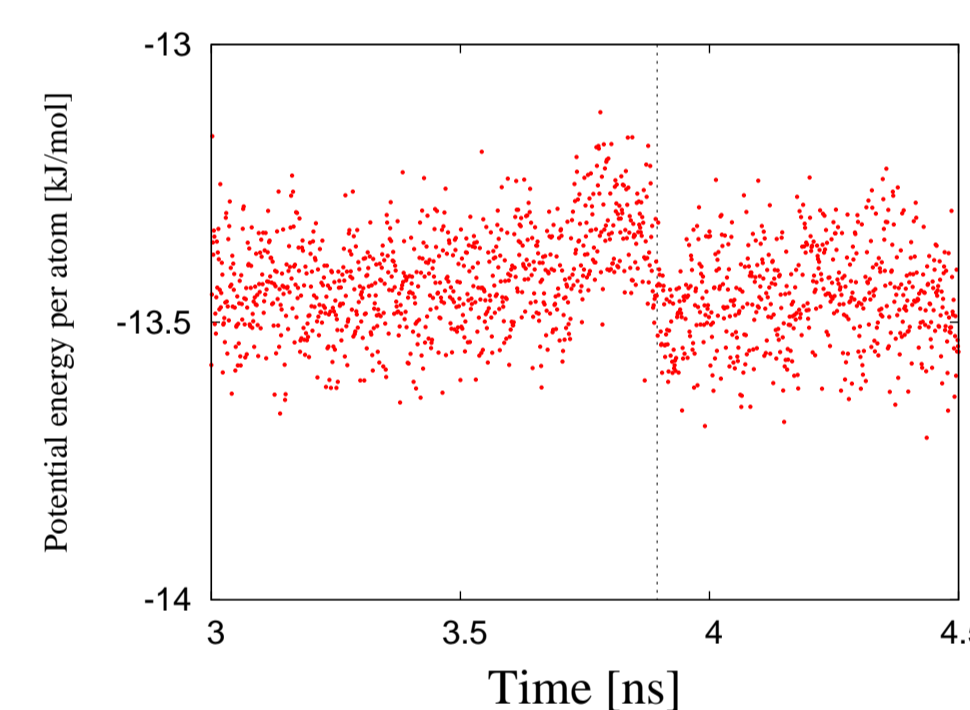


FIGURE 4: Potential energy per atom around the second fragmentation from $z = 10$ to 9 for the simulation in Figs. 1 and 2. The vertical dotted line shows the time of the fragmentation.

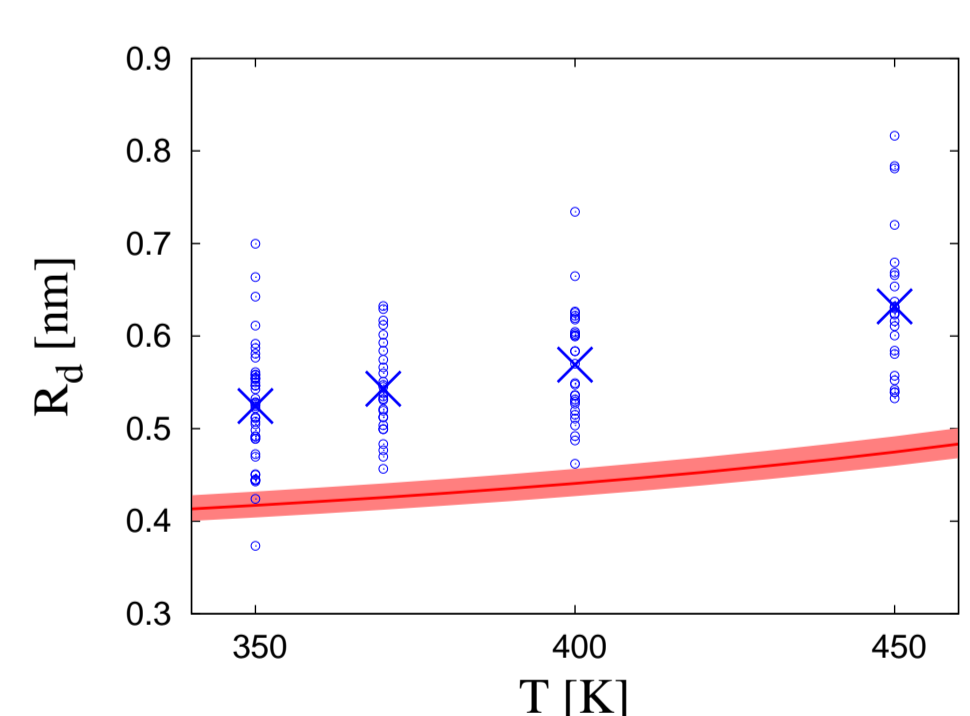


FIGURE 5: Radius of the daughter droplets, R_d , with a single charge $z = 1$. The open circles correspond to the results for each fragmentation event, and the cross marks are the averaged values. The solid line is the Born radius R_B .

T [K]	R_d [nm]	R_B [nm]	N_d	N_h
350	0.524	0.4168	18 ± 8.3	7.32
370	0.543	0.4253	19 ± 5.5	
400	0.569	0.4405	22 ± 7.2	7.34
450	0.632	0.4744	30 ± 8.7	7.26

TABLE 1: R_d , the Born radius R_B , the number of water molecules in daughter droplet N_d and the hydration number N_h for Cl^- .

Ion Evaporation Mechanism (IEM)

IEM[10] has been extended by taking into account the dielectric medium[18, 8] and curvature effects[19, 20] as

$$\Delta = \Delta^\circ - \frac{e^2}{8\pi\epsilon_0 R} \left\{ 1 + 2F(z-1) \right\} - \frac{8\pi\gamma R_d^3}{3R}, \quad (4)$$

where Δ° is given by Eq. (2), the second term is the charge correction and the third term is the curvature correction. $F(z)$ is a known function coming from the maximization of electrostatic energy[8].

At the fragmentation for the droplet with z ions, the critical size R^* is given by the critical energy Δ^* as

$$R^*(z) = \Gamma \left\{ F(z-1) + \alpha \right\}, \quad \Gamma = \frac{4R_B}{\frac{2}{x} + x^2 - 3g^*}, \quad \alpha = \frac{1}{2} + \frac{x^3}{6}, \quad (5)$$

where $x = R_d/R_B$ and $g^* = \Delta^*/\Delta G_S^\circ$. The fitting works well, but the physical interpretation is puzzling: α should be larger than $1/2$, but the simulations suggest that α is less than $1/2$. This is also observed in the experimental results [19, 21]. Furthermore, the energy Δ would give R_d with a certain dependency on z , while the results of R_d show no systematic z -dependence.

Simplified IEM

We take a simpler model without curvature correction

$$\Delta = \Delta^\circ - \frac{e^2}{8\pi\epsilon_0 R} \left\{ 1 + 2F(z-1) \right\}. \quad (6)$$

The results are shown in Fig. 3 with blue lines. This model gives R_d without z -dependence, therefore, consistent with the simulations. From the fitting parameter Γ , we have the activation energies decreasing as T becomes higher.

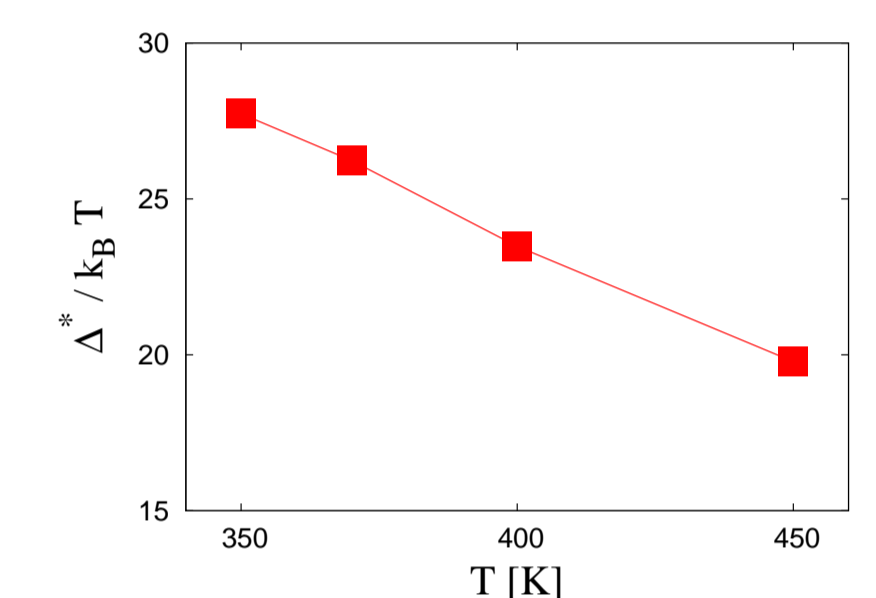


FIGURE 6: Activation energies $\Delta^*/k_B T$ based on the simplified IEM (6).

Conclusions

By constant-temperature MD simulations, the mechanism of ion fragmentation of charged aqueous nanodroplets has been examined. The solvent evaporation is taken into account directly and sequences of fragmentation events are observed. The critical radius $R^*(z)$ and size of the daughter droplets R_d are estimated directly.

- Minimum values of R_d and N_d are close to the Born radius R_B and the hydration number N_h of the ion, respectively.
- The critical radius $R^*(z)$ are compared with Rayleigh’s model and both improved and simplified ion evaporation models.
- We have decline the Rayleigh theory because the assumptions in the theory do not hold for the conditions of the simulations.
- For the improved IEM, it is found that the parameter related to the curvature correction are unphysical. Experimental data also give the same problematic behavior.
- The simplified IEM is introduced by eliminating the curvature correction. This model gives no z -dependence on R_d , which is consistent with the findings of simulations.
- The fitting of $R^*(z)$ with the simplified IEM is fairly good. It also gives activation energies that are positive and decrease with increase in temperature.

Acknowledgments

SC thanks the Natural Sciences and Engineering Research Council of Canada (NSERC) for funding this research and NSERC and Canada Foundation for Innovation (CFI) for a grant that allowed us to have the computing facilities used for the computations in this project. The authors thank Professor Lars Konermann for helpful discussions.

References

- [1] L. Rayleigh, *Phil. Mag.* **14**, 184 (1882).
- [2] *Electrospray Ionization Mass Spectrometry*, edited by R. B. Cole (Wiley-Interscience, New York, 1997).
- [3] J. B. Fenn *et al.*, *Science* **246**, 64 (1989).
- [4] P. Kebarle and M. Peschke, *Anal. Chim. Acta* **406**, 11 (2000).
- [5] J. B. Fenn, *Angew. Chem. Int. Ed.* **42**, 3871 (2003).
- [6] J. B. Fenn *et al.*, in *Biochemical and Biotechnological Applications of Electrospray Ionization Mass Spectrometry*, edited by A. P. Snyder (American Chemical Society, Washington, D.C., 1996).
- [7] P. Kebarle and M. Peschke, *Anal. Chim. Acta* **406**, 11 (2000).
- [8] M. Gamero-Castaño and J. Fernández de la Mora, *Anal. Chim. Acta* **406**, 67 (2000).
- [9] M. Dole *et al.*, *J. Chem. Phys.* **49**, 2240 (1968).
- [10] J. V. Iribarne and B. A. Thomson, *J. Chem. Phys.* **64**, 2287 (1976).
- [11] H. J. C. Berendsen, D. van der Spoel, and R. van Drunen, *Comp. Phys. Comm.* **91**, 43 (1995).
- [12] E. Lindahl, B. Hess, and D. van der Spoel, *J. Mol. Mod.* **7**, 306 (2001).
- [13] H. J. C. Berendsen, J. R. Grigera, and T. P. Staatsma, *J. Phys. Chem.* **91**, 6269 (1987).
- [14] J. Chandrasekhar, D. C. Spellmeyer, and W. L. Jorgensen, *J. Am. Chem. Soc.* **106**, 903 (1984).
- [15] M. L. Connolly, *J. Am. Chem. Soc.* **16**, 1118 (1985).
- [16] <http://dasher.wustl.edu/tinker/>.
- [17] IAPWS Release (1994).
- [18] I. G. Loscertales and J. Fernández de la Mora, *J. Chem. Phys.* **103**, 5041 (1995).
- [19] M. Gamero-Castaño and J. Fernández de la Mora, *J. Mass Spectrom.* **35**, 790 (2000).
- [20] M. Labowsky, J. B. Fenn, and J. Fernández de la Mora, *Anal. Chim. Acta* **406**, 105 (2000).
- [21] B. K. Ku and J. Fernández de la Mora, *J. Phys. Chem. B* **109**, 11173 (2005).